SUPPLEMENTARY INFORMATION

SLX4 contributes to telomere preservation and regulated processing of telomeric joint molecule intermediates

Jaya Sarkar[a], Bingbing Wan[b,c], Jinhu Yin[a], Haritha Vallabhaneni[a], Kent Horvath[a], Tomasz Kulikowicz[a], Vilhelm A. Bohr[a], Yanbin Zhang[d], Ming Lei[b,1], and Yie Liu[a,1]

[a]Laboratory of Molecular Gerontology, National Institute on Aging/National Institute of Health, 251 Bayview Blvd, Baltimore, MD 21044, USA. [b]National Center for Protein Science Shanghai, State Key Laboratory of Molecular Biology, Institute of Biochemistry and Cell Biology, Shanghai Institutes for Biological Sciences, Chinese Academy of Sciences, 333 Haike Road, Shanghai 200031, China. [c]Department of Biological Chemistry, University of Michigan Medical School, 1150 W. Medical Center Drive, Ann Arbor, MI 48109, USA. [d]Department of Biochemistry and Molecular Biology, University of Miami Miller School of Medicine, Miami, FL 33136, USA.

[1]Correspondence: Y.L. (liuyie@mail.nih.gov) or M.L. (leim@sibcb.ac.cn)

EXTENDED MATERIALS AND METHODS

Protein expression and purification. The $SLX1_{WT}$-$SLX4_{SBR}$ and $SLX1_{E82A}$-$SLX4_{SBR}$ complexes were expressed and purified as described in (1). TRF1 and TRF2 were expressed in E. coli BL21 (DE3) cells using a pET28a vector that contained a Sumo protein fused at the N-terminus after the His_6 tag. Proteins were purified via Ni-NTA (Qiagen) metal affinity chromatography, followed by Mono-Q ion exchange column chromatography. Finally the proteins were passed through HiLoad 200 Superdex gel filtration column (GE Healthcare). $TRF2_{TRFH}$ was purified as described in (1). The BLM gene was PCR-amplified from MegaMan Human Transcriptome Library (Agilent Technologies) using primers: hBLM-NotI-6xHis-F, 5'-GGAATTGCGGCCGCATGTCTCATCACCATCACCATCACGCTGCTGTTCCTCAAAATA ATCTAC-3' and hBLM-FLAG-blns-R, 5'-CTTATCGTCGTCATCCTTGTAATCTGAGAATGCATATGAAGGCTTAAGA-3', incorporating sequences encoding hexahistidine (6xHis) and FLAG tags at the 5' and 3' termini, respectively. The PCR product was digested with NotI, phosphorylated with PNK, and ligated into NotI/SmaI digested pFastBac1-InteinCBDAla vector, producing the 6xHis-BLM-FLAG/pFastBac1-InteinCBDAla construct. Generation of recombinant baculoviruses, protein expression and purification were carried out as previously described (2).

Cell culture, antibodies, and gene knockdown. Human cells were obtained from ATCC or from Dr. Titia de Lange (3). Cells were cultured in high glucose DMEM supplemented with 10% FBS at 37ºC in 5% CO_2. GenJet and pepmute (Signagen) transfection reagents were used for transient transfections of plasmids bearing respective protein constructs and small interfering RNA (siRNA), respectively. Rabbit anti-SLX4 antibody (against residues 660–869) was generated as described in (1). All other antibodies were commercially procured [anti-β-Actin (A5441, Sigma), anti-HA (H3663, Sigma; 3F10, Roche), anti-Myc (sc-14 and sc-789, Santa Cruz Biotechnology), and anti-BLM (C-18, sc-7790, Santa Cruz Biotechnology)]. Small hairpin or interfering RNA (shRNA or siRNA) knockdown of SLX4 or BLM was achieved as described in (1, 4).

Cell synchronization and cell cycle analysis. Cells were synchronized in specific phases of the cell cycle via double thymidine block. Cells were grown to 40% confluency. Medium containing 10% FBS and 2 mM thymidine (Sigma-Aldrich) was added and incubated for 18 hours at 37°C. Cells were then washed twice with PBS and grown at 37°C in medium containing 10% FBS for 9 hours and then in medium containing 10% FBS and 2mM thymidine for another 18 hours. After double-thymidine exposure, cells were washed twice with PBS, incubated in regular medium, harvested at different time points. For cell cycle analysis after DNA damage treatment, cells were harvested after respective treatment and fixed. Finally, for flow cytometric analyses, cells were stained with 0.1 mg/ml Propidium iodide (Sigma) in 0.6% Triton-X in PBS and analyzed using BD Accuri C6 flow cytometer.

Chromatin Immunoprecipitation. ChIP was performed as described previously (5) with minor modifications. Briefly, sheared chromatin (about ~500 bp) was incubated with 3 µg of antibodies [rabbit polyclonal anti-TRF2 (5) or rabbit anti-SLX4 (1) and Dynabeads Protein G

(Invitrogen)]. The precipitated DNA was then eluted and analyzed by dot-blotting using radiolabeled probes specific for telomeric sequence or Alu sequence.

Co-immunoprecipitation. The assay was performed as described in (1). Briefly, human U2OS cells (1 x 10^6 cells/mL) were transfected with two independent vectors containing Myc-SLX1 and HA-SLX4. 48 hours post transfection cells were resuspended in 800 µL lysis buffer (50 mM Tris-HCl, pH 7.5, 150 mM NaCl, 0.5% Triton-X-100. 0.5 mM EDTA, 10% glycerol, and protease inhibitor cocktail from Roche) and incubated with gentle rocking at 4 °C for 1 hr. After spinning down the cell debris, SLX1-SLX4 protein complex was co-immunoprecipitated from the supernatant incubating cell lysate with 50 µL magnetic Dynabeads protein G (Invitrogen) conjugated with anti-HA antibody at 4 °C for 2 hr. Protein complex-bound bead suspension was then used in the nuclease assays.

Oligonucleotide-based assembly of telomeric substrates. Oligonucleotides used in this study were synthesized and purified (Loftstrand Labs) (Table S1A). The constituent oligonucleotides of each substrate are mentioned in Table S1B. Respective oligonucleotides (10 pmoles) were labeled at the 5'-end using [^{32}P]-γ-ATP and T4 polynucleotide kinase according to manufacturer's protocol. Oligonucleotides 1 (radiolabeled) and 2 were annealed in 1 M NaCl by heating to 95 °C for 5 min, followed by slow cooling from 65 °C to 25 °C, to assemble the splayed arm substrate. The 3'-flap substrate was assembled by first annealing oligonucleotides 4 and 2 (2.5:1) in an annealing buffer (10 mM Tris-HCl, pH 8.0 and 50 mM NaCl) by incubating at 95 °C for 5 min, followed by slow cooling from 65 °C to 25 °C. The above annealed mixture was set up for a second annealing with radiolabeled oligonucleotide 1 by incubating at 37 °C for 2 hrs, followed by slow cooling to 25 °C. The 5'-flap substrate was assembled by first annealing oligonucleotide 3 and radiolabeled oligonucleotide 1 (5:1) in the annealing buffer by incubating at 95 °C for 5 min, followed by slow cooling from 65 °C to 25 °C. The above annealed mixture was set up for a second annealing with oligonucleotide 2 by incubating at 37 °C for 2 hrs, followed by slow cooling to 25 °C. The replication fork substrate was assembled by first setting up two independent annealing reactions (labeled oligonucleotide 1 and oligonucleotide 3; and oligonucleotides 2 and 4). These two separate annealing reactions were then mixed and incubated at 37 °C for 2 hrs, followed by slow cooling to 25 °C. The D-loop substrate labeled on the DL-IV strand was assembled as described in (6). The D-loop substrate labeled on the DL-T strand was assembled by first annealing oligonucleotides 9 and 11 (2:1) by incubating at 95 °C for 5 min and then 60 °C for 10 min. Radiolabeled oligonucleotide 10 was added to this annealing mixture, and incubated at 60 °C for 1 hr, followed by slow cooling to 25 °C. Similarly, the D-loop substrate labeled on DL-B strand was assembled by first annealing oligonucleotide 9 and radiolabeled oligonucleotide 11 (2:1), followed by addition of oligonucleotide 10. All substrates were purified using microspin G-25 spin columns (GE Healthcare), and verified for correct assembly via native gel electrophoresis.

Nuclease cleavage assays and TRF2/TRF1 protection assays. SLX1-dependent nuclease reactions were performed as described in (1). Briefly, the reactions included 0.5 nM model telomeric substrates constructed from oligonucleotides in appropriate reaction buffer and were initiated by respective enzyme(s) (purified or immunoprecipitated) in concentrations as specified, followed by incubation at 37 °C for 30 min. Reactions were stopped and deproteinized at specified time points with stop buffer. BLM and SLX1-SLX4 dependent reactions contained both enzymes premixed (at specified concentrations), followed by initiation with radiolabeled substrate. Reaction products were analyzed by 10% native or 14% denaturing polyacrylamide

gel electrophoresis. Dried gels were exposed to a BAS-phosphorimager screen, and images scanned using a Typhoon phosphorimager (GE Healthcare). Intensities of product bands were quantified using ImageQuant TL software (GE Healthcare).

REFERENCES

1. Wan B, *et al.* (2013) SLX4 assembles a telomere maintenance toolkit by bridging multiple endonucleases with telomeres. *Cell Rep* 4(5):861-869.
2. Tadokoro T, Kulikowicz T, Dawut L, Croteau DL, & Bohr VA (2012) DNA binding residues in the RQC domain of Werner protein are critical for its catalytic activities. *Aging (Albany NY)* 4(6):417-429.
3. Smogorzewska A, *et al.* (2000) Control of human telomere length by TRF1 and TRF2. *Mol Cell Biol* 20(5):1659-1668.
4. Garner E, Kim Y, Lach FP, Kottemann MC, & Smogorzewska A (2013) Human GEN1 and the SLX4-associated nucleases MUS81 and SLX1 are essential for the resolution of replication-induced Holliday junctions. *Cell Rep* 5(1):207-215.
5. Yang D, *et al.* (2011) Human telomeric proteins occupy selective interstitial sites. *Cell Res* 21(7):1013-1027.
6. Opresko PL, *et al.* (2004) The Werner syndrome helicase and exonuclease cooperate to resolve telomeric D loops in a manner regulated by TRF1 and TRF2. *Mol Cell* 14(6):763-774.

SUPPLEMENTARY FIGURES

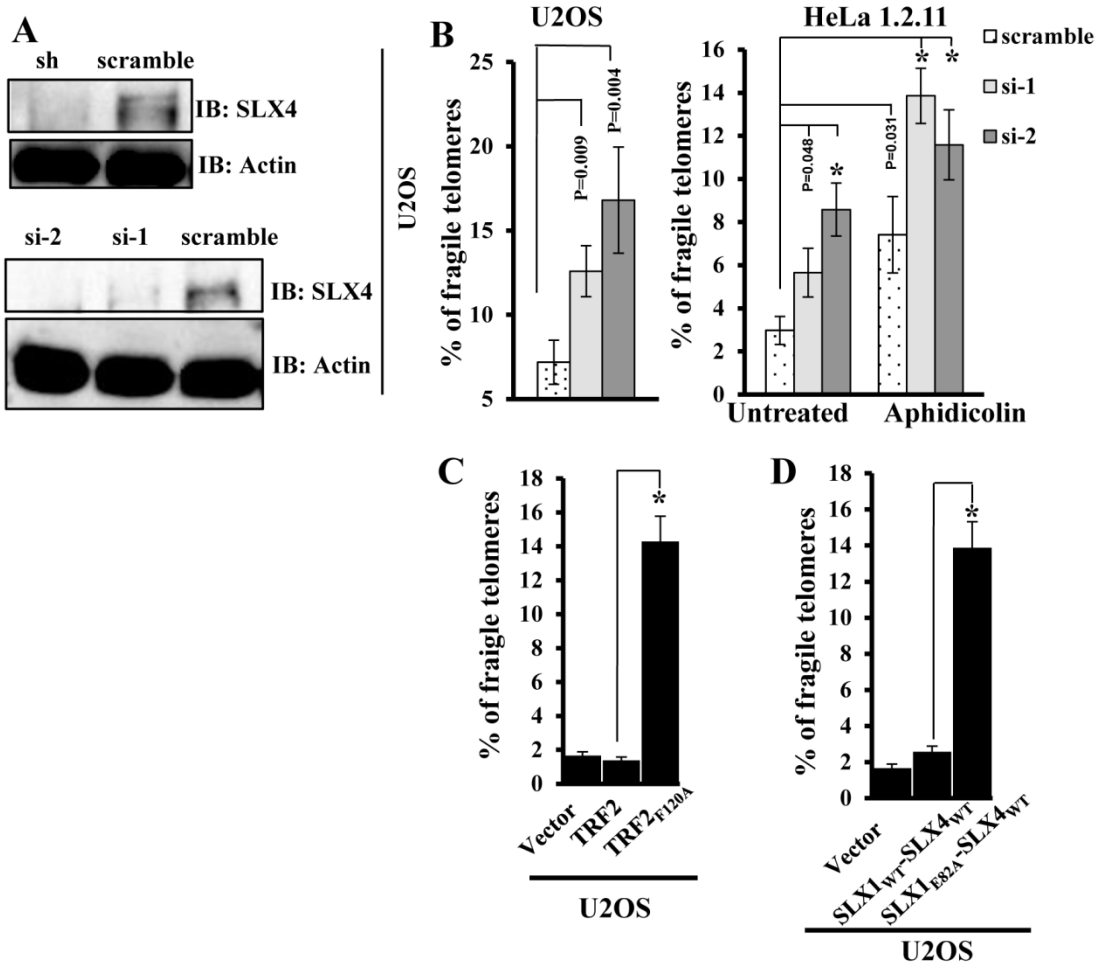

Figure S1. Dissection of the SLX4 complex in preventing telomere fragility. (A) Representative western blot image showing transient (siRNA-mediated, si-1 or si-2) or stable (shRNA-mediated) depletion of SLX4 in U2OS cells. Actin is shown as loading control. (B) U2OS (left) or HeLa 1.2.11 (right) cells transiently depleted of SLX4 (by two different siRNAs, si-1 and si-2) exhibit increased fragile telomeres, as compared to cells transiently transfected with scramble siRNA. Treatment with 0.5 μM aphidicolin exacerbated fragile telomeres in HeLa 1.2.11 cells (right). (C) Percentage of fragile telomeres in U2OS cells transiently transfected with wild-type TRF2 or $TRF2_{F120A}$ mutant that does not interact with SLX4. (D) Frequency of fragile telomeres in U2OS cells transiently transfected with wild-type or nuclease-dead SLX1-SLX4 fusion proteins. Error bars represent standard deviation from three independent experiments of each genotype (30 metaphases / genotype / experiment). Frequency of fragile telomeres was compared between two groups using a student's t test. * $p<0.0001$.

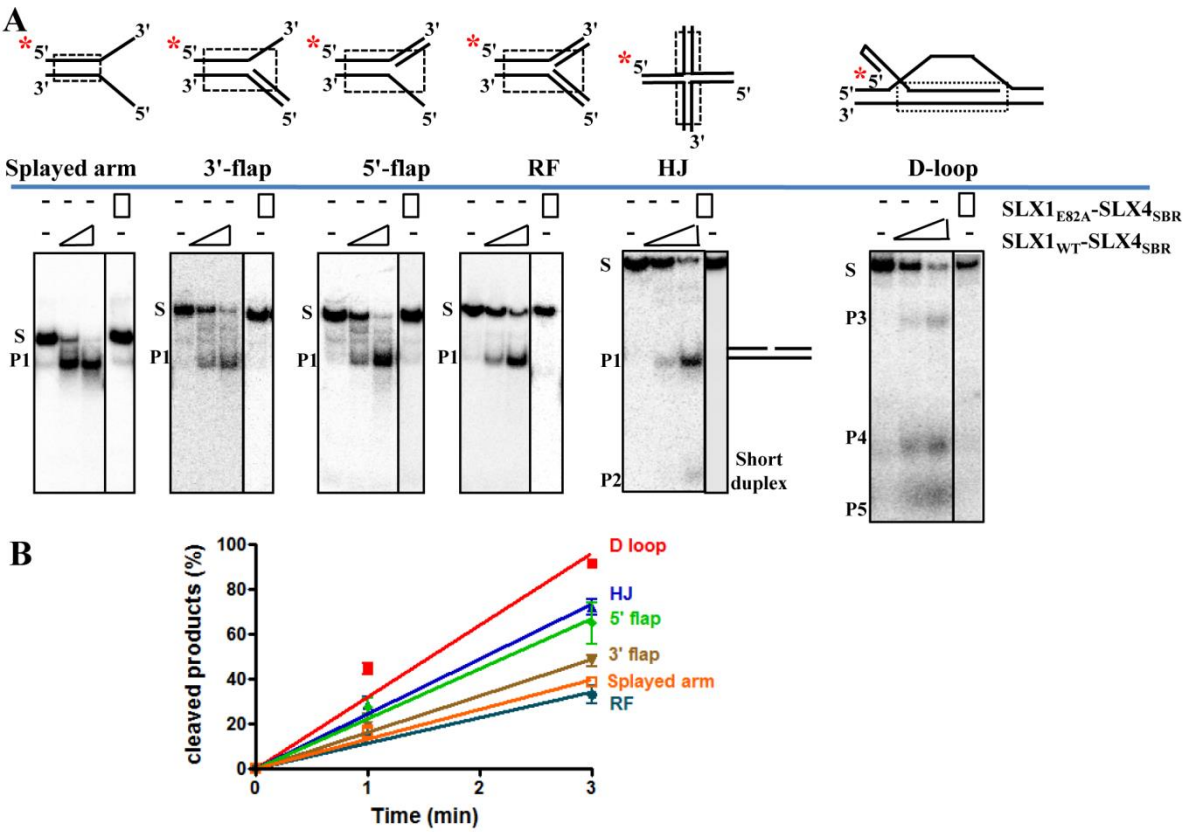

Substrate	RF	Splayed arm	3'-flap	5'-flap	HJ	D-loop
k_{obs} (min^{-1})	11.5 ± 0.9	13.2 ± 0.6	16.3 ± 0.9	22.3 ± 1.6	24.4 ± 0.9	32.6 ± 1.6

Figure S2. The SLX1-SLX4 complex nucleolytically processes a wide array of branched telomeric substrates *in vitro*. (A) Representative native gel images of enzyme titration, (B) time course of reaction extent and observed rate constants of nucleolytic activity of purified $SLX1_{WT}$-$SLX4_{SBR}$ *in vitro*. The nuclease-dead purified $SLX1_{E82A}$-$SLX4_{SBR}$ mutant complex is shown as negative control for all the substrates. Dashed boxes signify telomeric regions on the model oligonucleotide-based substrates, which were 5'-[^{32}P]-radiolabeled, as indicated by red asterisk. The respective substrate is indicated as S and the nicked duplex product as P1. An additional short duplex product is marked as P2 for the HJ substrate. Cleavage products of the D-loop substrate are marked as P3, P4, and P5. For all experiments, 0.5 nM substrate was used. Nuclease reactions contained 0.5 or 1 nM $SLX1_{WT}$-$SLX4_{SBR}$ or 1 nM $SLX1_{E82A}$-$SLX4_{SBR}$ purified enzyme complex. For time course analysis, reactions were initiated with 0.5 nM wild-type enzyme complex, aliquots collected and reaction stopped at different time points. Error bars were calculated from triplicate data. Observed rate constants (k_{obs}) are shown in the table. The gel images were re-constructed by omitting irrelevant lanes for clarity. Separating lines between lanes indicate that the lane was from a different gel or a different exposure of the same gel.

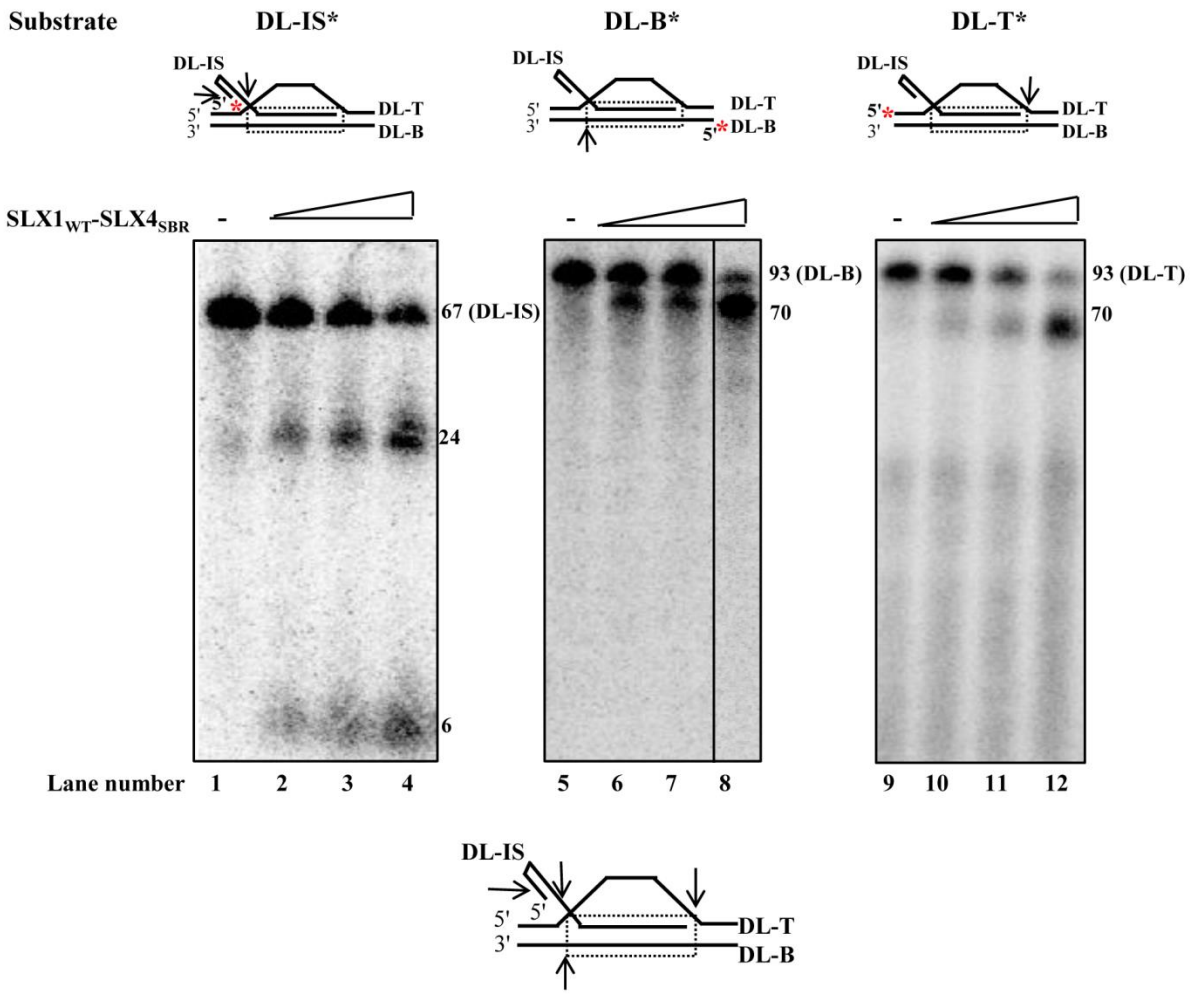

Figure S3. Pattern of SLX1-SLX4 nuclease module-sponsored processing of telomeric D-loop *in vitro*. Representative denaturing gels depicting cleavage of the model telomeric D-loop substrate radiolabeled (indicated by asterisk) on any of the three strands, DL-IS (left panel, lanes 1-4), DL-B (center panel, lanes 5-8), and DL-T (right panel, lanes 9-12). The center panel has been reconstructed from the same gel, by omitting irrelevant lanes for clarity, as depicted by the separating line between lane 7 and 8. The dashed boxes denote telomeric sequences on the DNA substrates. A summary of the SLX1 cleavage pattern on the telomeric D-loop is shown (bottom). Nuclease cleavage reactions contained 0.5 nM substrate and 0 to 2 nM of purified $SLX1_{WT}$–$SLX4_{SBR}$ complex. The numbers on the right side of each gel represent approximate sizes of the cleaved products. Beside each gel, the uncleaved radiolabled oligonucleotides are also indicated as DL-IS (67-mer), DL-B (93-mer), and DL-T (93-mer) for the respective D-loop substrate.

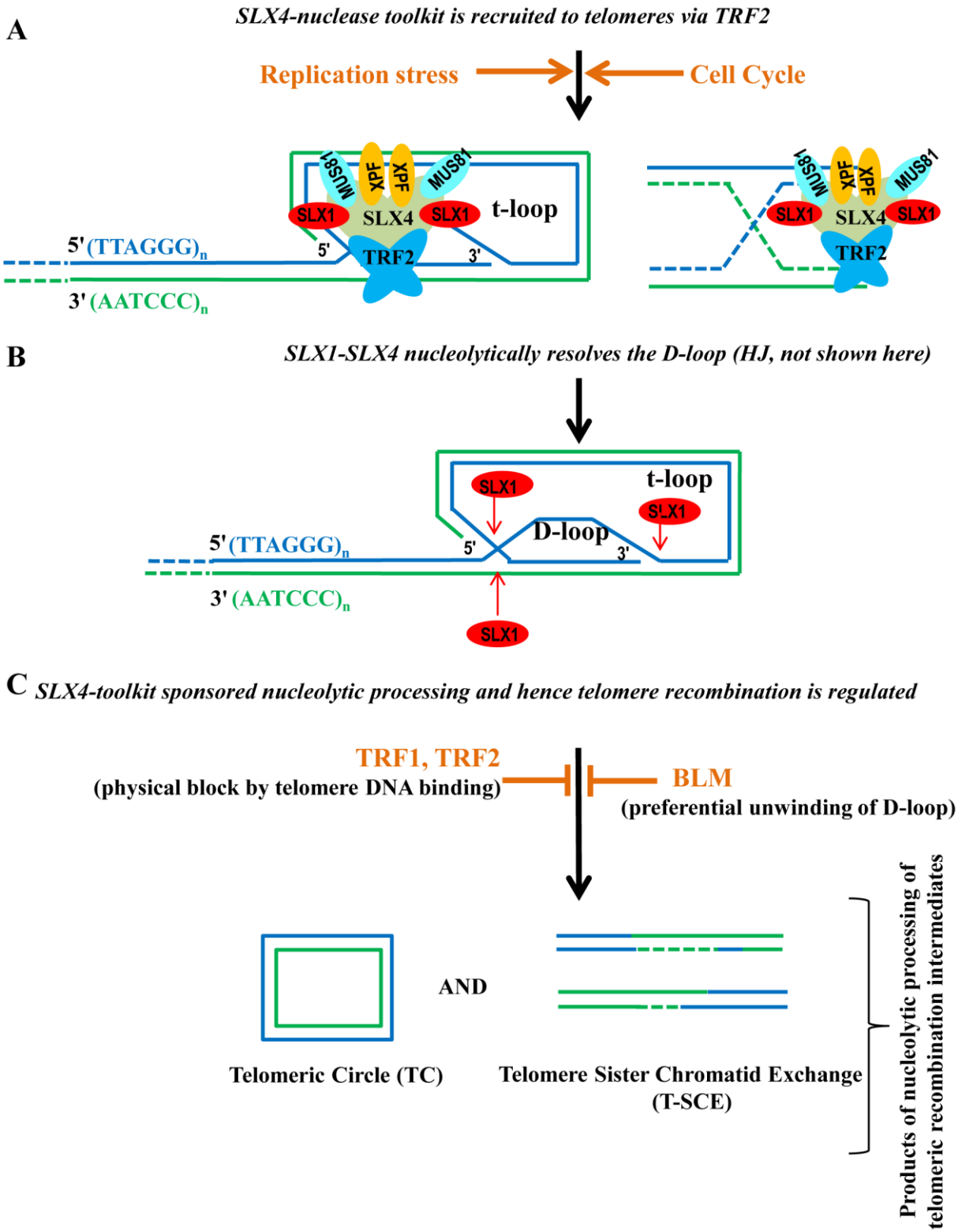
A
SLX4-nuclease toolkit is recruited to telomeres via TRF2
Replication stress
Cell Cycle
MUS81
XPF
XPF
MUS81
SLX1
SLX4
SLX1
t-loop
5'
3'
TRF2
5' (TTAGGG)n
3' (AATCCC)n
B
SLX1-SLX4 nucleolytically resolves the D-loop (HJ, not shown here)
SLX1
t-loop
SLX1
D-loop
5'
3'
5' (TTAGGG)n
3' (AATCCC)n
SLX1
C
SLX4-toolkit sponsored nucleolytic processing and hence telomere recombination is regulated
TRF1, TRF2
(physical block by telomere DNA binding)
BLM
(preferential unwinding of D-loop)
AND
Telomeric Circle (TC)
Telomere Sister Chromatid Exchange
(T-SCE)
Products of nucleolytic processing of
telomeric recombination intermediates

Figure S4. Model depicting recruitment, mechanism, and regulation of the SLX4-nuclease complex in telomere maintenance. (A) The SLX4-nuclease complex is recruited to telomeres via direct SLX4-TRF2 interaction. The telomeric association of SLX4 is regulated by cell cycle and replication stress. (B) At telomeres, the SLX1-SLX4 complex is required for processing of telomeric joint molecule intermediates, accomplished by nucleolytic incision in the intervening sequences by SLX1-SLX4. This leads to resolution of the D-loop and/or HJ, resulting in formation of extrachromosomal telomeric circles and/or T-SCE events *in vivo*. (C) SLX1-SLX4 nucleolytic activity at telomeres is negatively regulated by multiple factors - physical blocking by telomeric DNA-binding proteins TRF1 and TRF2 and preferential unwinding of the D-loop or non-crossover of telomere HJ by the helicase BLM. *In vivo*, a combination of these factors may ensure regulated nucleolytic processing of telomeric HR intermediates, and hence TC formation and T-SCE events.

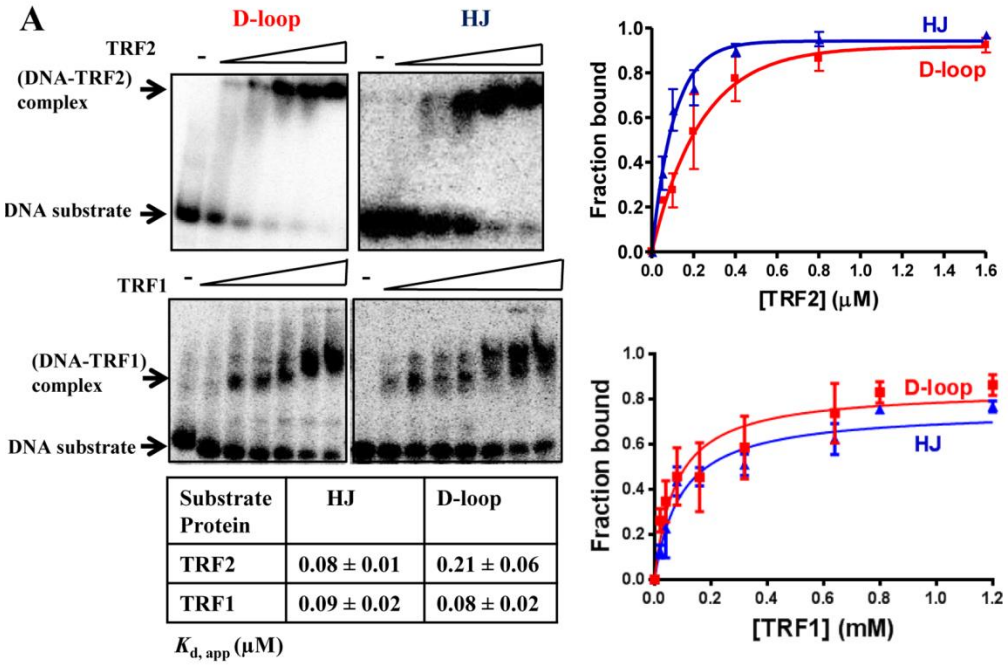

Substrate Protein	HJ	D-loop
TRF2	0.08 ± 0.01	0.21 ± 0.06
TRF1	0.09 ± 0.02	0.08 ± 0.02

$K_{d,\,app}$ (μM)

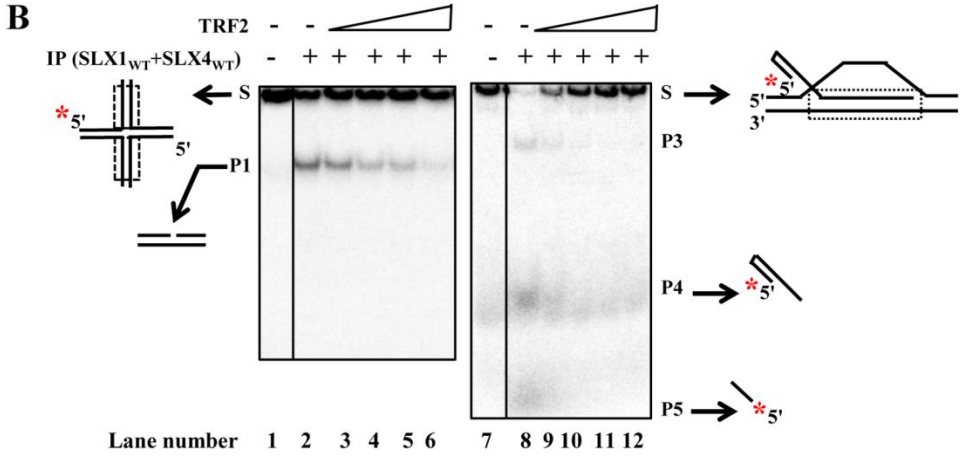

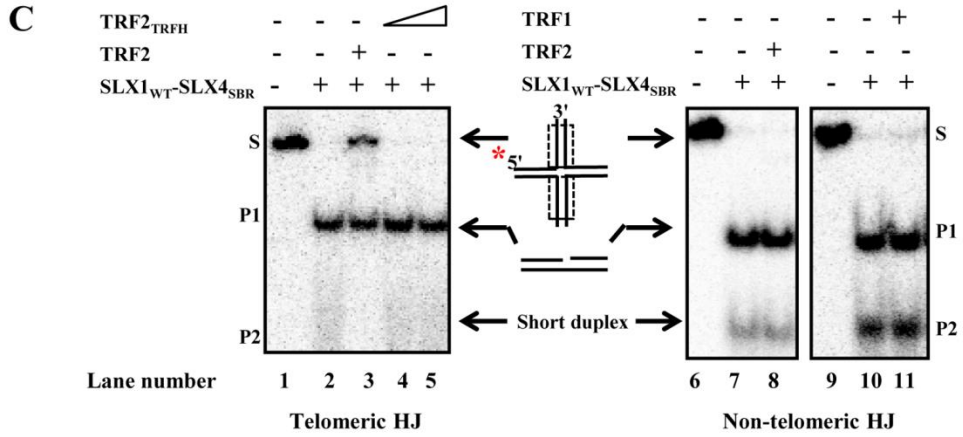

Figure S5. Telomere-binding proteins physically block access of SLX1-SLX4 nuclease module specifically to telomeric substrates. (A) Representative gel images (left) and quantification (right) of electrophoretic mobility shift assay showing comparable formation of DNA-protein complex for the telomeric D-loop and HJ substrates with either TRF2 or TRF1. The table shows the calculated apparent dissociation constants ($K_{D,app}$). Binding reactions contained 0.5 nM of respective substrate and 0 to 1.6 μM purified TRF2 or 0 to 1.2 μM purified TRF1. (B) TRF2 also limits nuclease activity of the immunoprecipitated ($SLX1_{WT}$ + $SLX4_{WT}$) complex on the telomeric HJ (lanes 1-6) and D-loop (lanes 7-12) substrate, as suggested by disappearance of the respective products. Reactions containing pre-bound TRF2 (0 to 60 nM) to respective telomeric substrate were initiated with 3 μL immuprecipitated ($SLX1_{WT}$ + $SLX4_{WT}$) complex. (C) Representative native gel images showing that $TRF2_{TRFH}$ does not protect telomeric HJ unlike full-length TRF2 (left, compare lanes 4 and 5 with lane 3) and that TRF1 and TRF2 do not protect non-telomeric HJ (right) from cleavage by purified $SLX1_{WT}$-$SLX4_{SBR}$ complex. Respective substrates were pre-bound with purified $TRF2_{TRFH}$ (0 to 30 nM), TRF1 (60 nM), or TRF2 (60 nM) on ice for 5 min, followed by addition of 0.5 nM purified $SLX1_{WT}$-$SLX4_{SBR}$ complex.

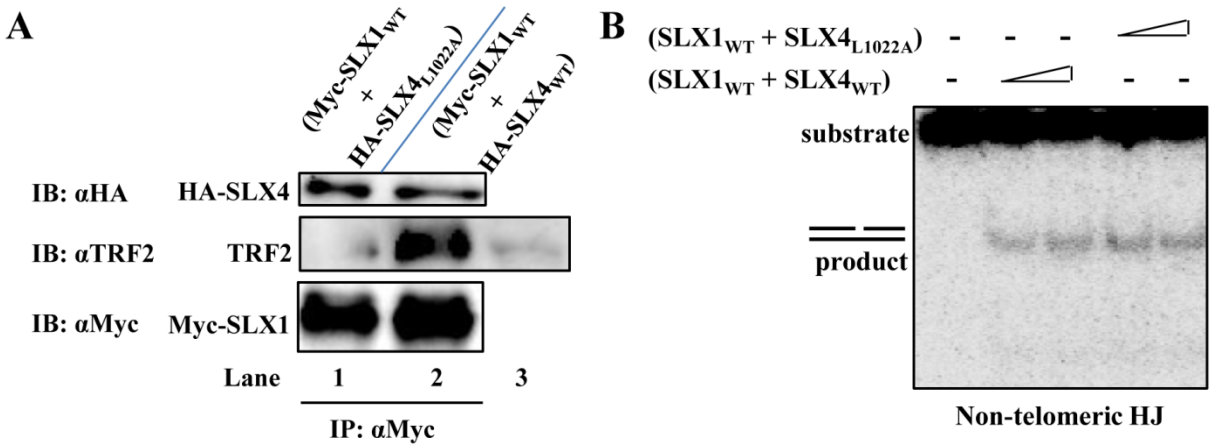

Figure S6. Nuclease activity of the SLX1-SLX4 module is independent of the SLX4-TRF2 interaction. (A) Western Blot analysis showing comparable levels of Myc-SLX1 and HA-$SLX4_{WT}$ or HA-$SLX4_{L1022A}$ in co-immunoprecipitated complexes. The wild type SLX4 complex (lane 2) shows more TRF2 pulled down as compared to the mutant SLX4 complex (lane 1). Myc-$SLX1_{WT}$ was transiently expressed together with HA-$SLX4_{WT}$ or HA-$SLX4_{L1022A}$. Each complex was co-immuprecipitated using anti-Myc antibody. Anti-Myc, anti-HA, and anti-TRF2 antibodies were used to probe for Myc-SLX1, HA-SLX4, and TRF2. Lane 3 depicts endogenous TRF2 detected in 2% of the input lysate used for the co-IPs. (B) Representative native gel image showing similar levels of nucleolytic processing of non-telomeric HJ by the co-immunoprecipitated wild type and mutant SLX4 complexes.

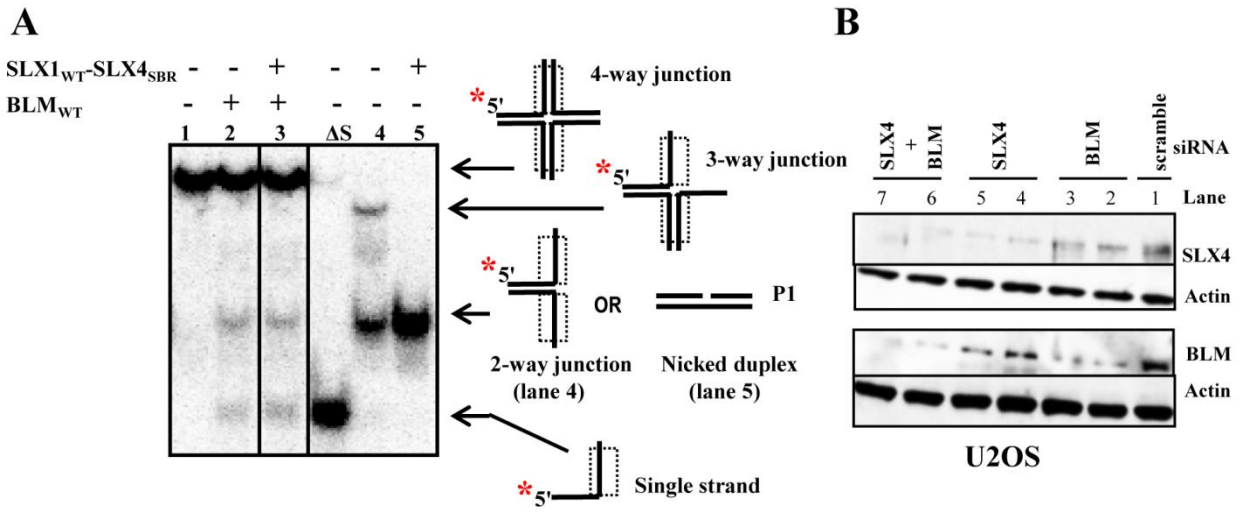

Figure S7. BLM subdues nucleolytic processing of telomeric HJ *in vitro*. (A) Representative native gel image showing unwound or nucleolytically cleaved telomeric HJs in the presence of purified BLM alone (lane 2), or $SLX1_{WT}$-$SLX4_{SBR}$ complex alone (lane 5), or both (lane 3). The heat-denatured substrate is indicated as ΔS. A mixture of the 3-way and 2-way species was loaded as a control in lane 4. The 4-way, 3-way, 2-way, and single-stranded species of the HJ substrate are indicated on the right. The nicked duplex product P1 has similar electrophoretic mobility as the 2-way HJ species. (B) Representative western blot showing transient (si-RNA-mediated) depletion of SLX4, BLM, or both in U2OS cells. Actin is shown as loading control.

Table S1A. Sequences of synthetic oligonucleotides used to assemble model telomeric substrates *in vitro*.

Name	Sequence
1	5'-GCGCTAGGCACGCGACTGGCGATCGGA$(CCCTAA)_6$ TGCTATCTGGCACTCAGTTCTA-3'
2	5'-CCTGGCATTCTCTATAAAGGTAG$(TTAGGG)_6$ TCCGATCGCCAGTCGCGTGCCTAGCG-3'
3	5'-CTAGAACTGAGTGCCAGATAGCA$(TTAGGG)_3$-3'
4	5'-$(CCCTAA)_3$CTACCTTTATAGAGAATGCCAG-3
5	5'-CAGATGGACATCTTTGCCCACGTTGACCCGAA$(TTAGGG)_4$CCATGGTAGCCC-3'
6	5'-GGGCTACCATGG$(CCCTAA)_4$TTGACATGCTGTCTAGAGACTATCGC-3
7	5'-GCGATAGTCTCTAGACAGCATGTCCG$(TTAGGG)_4$CAAGCGTCCGAG-3
8	5'-CTCGGACGCTTG$(CCCTAA)_4$CGCGGGTCAACGTGGGCAAAGATGTCCATCTG-3'
9	5'-CACCATCCAGTTCTCTTTTGAGAACTGGATGGTG$(TTAGGG)_4$TTAACGCTC-3
10	5'-CGTGACCAGGACGTGAGTCTCGAGTGCAGACC$(T)_{31}$ ACAATCATCCTGACTGCAGACCGAGCTTGA-3'
11	5'-TCAAGCTCGGTCTGCAGTCAGGATGATTGTGAGCGTTAA$(CCCTAA)_4$ TCTGCACTCGAGACTCACGTCCTGGTCACG-3

Table S1B. The constituent oligonucleotides of each substrate

Substrate	Constituent oligonucleotide
Splayed arm	1 and 2
3'-flap	1, 2, and 4
5'-flap	1, 2, and 3
Replication Fork	1, 2, 3, and 4
Holliday junction (HJ)	5, 6, 7, and 8
D-loop	9, 10, and 11